ADVANCES IN ATMOSPHERIC SCIENCES, VOL. 30, NO. 5, 2013, 1275–1286

Relationship between Cloud Characteristics and Radar Reflectivity Based on Aircraft and Cloud Radar Co-observations

ZONG Rong[1,2] (宗 蓉), LIU Liping*[2] (刘黎平), and YIN Yan[1] (银 燕)

[1] *China Meteorological Administration Key Laboratory for Atmospheric Physics and Environment, Nanjing University of Information Science and Technology, Nanjing* 210044

[2] *State Key Laboratory of Severe Weather, Chinese Academy of Meteorological Sciences, Beijing* 100081

(Received 7 May 2012; revised 18 November 2012; accepted 5 January 2013)

ABSTRACT

Cloud properties were investigated based on aircraft and cloud radar co-observation conducted at Yitong, Jilin, Northeast China. The aircraft provided *in situ* measurements of cloud droplet size distribution, while the millimeter-wavelength cloud radar vertically scanned the same cloud that the aircraft penetrated. The reflectivity factor calculated from aircraft measurements was compared in detail with simultaneous radar observations. The results showed that the two reflectivities were comparable in warm clouds, but in ice cloud there were more differences, which were probably associated with the occurrence of liquid water. The acceptable agreement between reflectivities obtained in water cloud confirmed that it is feasible to derive cloud properties by using aircraft data, and hence for cloud radar to remotely sense cloud properties. Based on the dataset collected in warm clouds, the threshold of reflectivity to diagnose drizzle and cloud particles was studied by analyses of the probability distribution function of reflectivity from cloud particles and drizzle drops. The relationship between reflectivity factor (Z) and cloud liquid water content (LWC) was also derived from data on both cloud particles and drizzle. In comparison with cloud droplets, the relationship for drizzle was blurred by many scatter points and thus was less evident. However, these scatters could be partly removed by filtering out the drop size distribution with a large ratio of reflectivity and large extinction coefficient but small effective radius. Empirical relationships of Z–LWC for both cloud particles and drizzle could then be derived.

Key words: aircraft, millimeter wavelength cloud radar, droplet size distribution, reflectivity, liquid water content

Citation: Zong, R., L. P. Liu, and Y. Yin, 2013: Relationship between cloud characteristics and radar reflectivity based on aircraft and cloud radar co-observation. *Adv. Atmos. Sci.*, **30**(5), 1275–1286, doi: 10.1007/s00376-013-2090-7.

1. Introduction

Clouds, with their global distribution, have a significant influence on the Earth-atmosphere energy budget; even a small change in cloud properties will affect radiative forcing (Slingo, 1990). Several critical microphysical properties of clouds, for instance the droplet size distribution (DSD), liquid water content (LWC), and the phase of cloud particles, determine their radiative properties (Sassen et al., 1999).

By providing detailed information on the temporal and spatial structures of cloud, *in situ* aircraft measurements have played an important role in advancing our understanding of cloud microphysical and dynamic processes. However, aircraft measurements are limited by both the high cost of performing the measurements and the small sampling volume. A modern aspect of the study of clouds has increasingly relied on remote sensing techniques, which monitor clouds with cost-effective and continuous measurements. Millimeter-wavelength cloud radar (MMCR), as one of the most important remote sensors, has become a powerful tool

*Corresponding author: LIU Liping, lpliu@cams.cma.gov.cn

to detect non- and weak-precipitating clouds because of their sensitivity to relatively small cloud droplets, low attenuation by atmospheric gases and insusceptibility to ground clutter (Kropfli and Kelly, 1996; Kollias et al., 2007).

Many observational studies have been carried out to characterize cloud properties by incorporating both aircraft and remote sensing measurements. Morales et al. (2004), for example, analyzed reflectivity from ice crystals within cirrus clouds and found that the reflectivity derived from radar and aircraft was similar when the aircraft was overflying the radar. By analyzing the microphysics of Arctic clouds from a synergetic aircraft-cloud radar observation, Lawson and Zuidema (2009) found the agreement between radar and aircraft data was reasonably good in terms of the reflectivity and derived microphysical parameters for the all-water and all-ice cases, but was much poorer in mixed-phase conditions. These features were also demonstrated by Hogan et al. (2006), who made comparisons between aircraft measurements and a 3-GHz radar.

The good agreement between radar and aircraft measurements supports the notion that radar data can be calculated from aircraft DSDs, and hence has a relationship with the microphysical properties of pure water and ice clouds. Numerous studies in the past have endeavored to realize the capability of radar to derive cloud microphysical characteristics, of which one traditional subject focuses on the ability of radar to diagnose precipitating clouds by setting a threshold on radar reflectivity factor. This is important since drizzle has a great impact on cloud morphology and associations with cloud microphysical and dynamical processes (Comstock et al., 2005). However, there seem to be large uncertainties in determining the threshold reflectivity, and a range of values has been used. From *in situ* DSD measurements for continental stratocumulus, Sauvageot and Omar (1987) put forward -15 dBZ as a threshold between precipitating and nonprecipitating warm clouds, and Chin et al. (2000) used this threshold for microphysical retrieval of continental stratiform clouds. Baedi et al. (2000) reported that stratocumulus clouds with reflectivities below a threshold of -20 dBZ are free of drizzle. This threshold was also employed by Frisch et al. (1995) to identify drizzle-free clouds, and they also found a radar reflectivity value of greater than -17 dBZ tends to be an indicator of the existence of drizzle droplets. Kogan et al. (2005) chose -17 dBZ as the reflectivity threshold to discriminate between nonprecipitating and precipitating clouds in their study.

Reflectivity factor (Z) and some cloud properties, such as LWC or effective radius (r_e), are proportional to the moments of DSDs. Relationships between these parameters can be expected by relating the different moments of DSDs. This is an empirical algorithm and is generally applied to clouds without drizzle or drizzle-free flight legs in precipitating cloud. Since in the Rayleigh regime the *in situ* reflectivity factor is proportional to the sixth moment of size spectra, while LWC is proportional to the third moment, a small population of drizzle drops will dominate the cloud reflectivity but have a weak influence on liquid water content, hence bring about a poor correlation between Z and LWC. From other points of view, the presence of drizzle droplets is even more frequent in cloud than its absence. However, a typical radar (without the Doppler spectrum data) cannot distinguish reflectivity due to cloud droplets from that due to drizzle particles. Consequently, it is of significance to retrieve a Z-LWC relation taking drizzle into consideration in order to estimate LWC from reflectivity alone. As noted in some studies (Krasnov and Russchenberg, 2005; Khain et al., 2008), although a Z–LWC relation presents more scattering when drizzle droplets exist, it still conforms to a power relation. Over past decades a number of relationships have been empirically proposed from airborne DSDs measurements in both marine and continental clouds (e.g. Sauvageot and Omar, 1987; Paluch et al., 1996; Fox and Illingworth, 1997; Baedi et al., 2000; Wang and Geerts, 2003). However, there has not yet been a consistent relationship between radar reflectivity factor and other properties of clouds reported in the literature. Such discrepancies are expected in response to different physical mechanisms that have critical influences on DSDs (Liu et al., 2008), and Sauvageot and Omar (1987) suggested taking into account cloud type for the determination of radar cloud parameter relationships.

In this paper we present results from an aircraft and MMCR co-observation campaign carried out in Yitong, Jilin Province, Northeast China. Data were collected on three days: 28 August, 29 August and 17 September 2010. An analysis of *in situ* cloud data and simultaneous radar observations is needed to evaluate the accuracy of aircraft-derived reflectivity. This paper also aims at providing an interpretation of cloud physical parameters from reflectivity.

The structure of the paper is organized as follows. Section 2 describes the instruments used in this study, and the method for data processing is presented in section 3. Section 4 evaluates the accuracy of the aircraft data by comparing the aircraft-derived reflectivity factors and coincident radar measurements. The threshold reflectivity factor between drizzle-free and with-drizzle cloud is estimated and empirical relationships between reflectivity factor and LWC are derived for both cloud and drizzle droplets in section 5. Fi-

nally, main conclusions are summarized in section 6.

2. Instruments and data

2.1 *In situ probe*

The cloud, aerosol and precipitation spectrometer (CAPS, Droplet Measurement Technologies Co. Ltd, USA), which has the same capabilities of conventional Particle Measurement System (PMS) particle probes, was adopted in this observation to measure the cloud parameters. CAPS is composed of five sensors: a cloud and aerosol spectrometer (CAS), cloud imaging probe (CIP), liquid water content detector, an air speed sensor, and a temperature probe (Baumgardner et al., 2001). The two principal instruments available here were the CAS and CIP probes.

The CAS instrument determines particle size by measuring the forward-scattered light (4°–12°) from a particle passing through a laser beam. This technique is similar to that of the widely used FSSP(Forword Scattering Spectrometer Probe). Moreover, the CAS possesses an additional set of optics and detectors to measure the scattered light in the backwards direction (168°–176°). Such information provides the potential to determine the phase (liquid or solid) and the real component of a spherical particle's refractive index. The CAS covers sizes ranging from 0.51 to 50 μm in diameter, which is usually divided into 30 bins.

The CIP relies on the same optical imaging techniques as in PMS 2D-OAP(Two Dimensional Optical Array Probe). In the CIP probe, there is a 64-element photosensitive diode array illuminated by a laser beam. When a particle passes through the laser beam, its shadow is projected on the diode array. According to the number of shadowing diodes, the particle's size is determined. As the outer two diodes (i.e. one and sixty-four) are rejected from the sizing counting, the CIP detects particles with diameters between 12.5 to 1550 μm with a 25-μm resolution. The sampling period of both probes was set to one second, which was a distance of about 60 m on the flight path. A series of housekeeping channels on the CIP provide meaningful digital values, such as relative humidity (RH), which are calculated from analog-to-digital converter values.

2.2 *MMCR*

The millimeter-wavelength radar used in this study is developed by the State Key Laboratory of Severe Weather (LaSW), Chinese Academy of Meteorological Sciences (CAMS). It is a fully coherent radar operating at a frequency of 35 GHz (Ka-band and 8.66-mm wavelength), with a 0.44° beamwidth and 30-m vertical resolution. In the Rayleigh scattering regime (scattering by particles whose diameters are much smaller than the radar wavelength λ) the radar backscattering cross section is proportional to λ^{-4}. So, the cloud radar has an excellent sensitivity to small hydrometeors (Kollias et al., 2007). Besides, owing to its shorter wavelength, the cloud radar is negligibly interfered by the Bragg scatter and ground clutter which aggravate the centimeter radar to interpret the backscattered returns from clouds. The narrow beamwidth and fine spatial resolution reduce its sampling volume. The small sampling volume decreases the effects of the Doppler spectrum broadening caused by turbulence (Kollias et al., 2002). Furthermore, this radar is equipped with dual polarization, and thus can provide information about the phase of particles in clouds. Its range gate number is 500, but usually the measurements for the first eighteen gates are invalid. The maximum detectable height is 14 460 m. Four pulse width options are available (0.3 μs, 1.5 μs, 20 μs and 40 μs), which give this radar an advantage in detecting different kinds of clouds (Zhong et al., 2011). A narrow pulse width mode is suitable for observing low clouds, while a long pulse width mode provides high sensitivity and can detect optically thin clouds, such as cirrus. All of these factors make this radar an ideal tool for cloud detection.

3. Data processing

Continuous DSDs can be obtained by combining the CAS and CIP particle data. An example of a completed DSD is shown in Fig. 1. The triangles represent

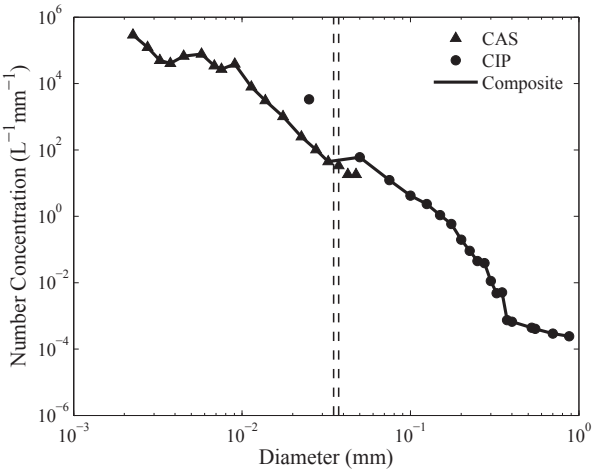

Fig. 1. An example of a combined DSD collected for a 60-s period on 17 September 2010. The spectrum of the combined DSD is expressed by the blue line. The triangles and circles denote the CAS and CIP data, respectively. The last three bins in CAS and the first bin in CIP is eliminated in the combined DSD. The two vertical dashed lines indicate the division that is from 35 to 37.5 μm between CAS and CIP.

the CAS data, and the circles the CIP data. The composition of the combined DSD was based on three considerations. Firstly, the CAS measurements beginning with 2 μm was chosen to represent cloud droplets in light of FSSP's size range (2–47 μm), and thus the first twelve bins of CAS were rejected. Taking into consideration that the first bins of cloud probes are unreliable, the data that came from the first bin of CIP were also discarded. Due to the size ranges of each probe, there was inevitably a breakpoint (or an overlap) in the combined DSD, and it was hoped that this would be as narrow as possible. As a result, the total spectrum was composed of two parts: the front segment formed by fifteen bins starting from the thirteenth in CAS; and the second half consisting of the CIP data covering the second to the sixty-second bin. The breakpoint, lying between 35 and 37.5 μm, is indicated by two dashed vertical lines in Fig. 1. The combined droplet spectrum was then used to calculate the parameters, such as total number concentration, reflectivity factor, and LWC.

Three rules were employed to determine a valid record in our study. Firstly, the total number concentration of droplets needed to be more than 10 cm^{-3}. Next, the liquid water content calculated from combined DSDs was required to be above 0.001 g m^{-3} in order to avoid the impact of aerosols. Finally, the records had to be in a series of at least five successive seconds. After that, the data were divided into many legs, and then the legs with less than 20 records were purged. The flight pattern and a series of valid legs are presented in Fig. 2 for the flight on 28 August 2010. The black line illustrates the track of the plane, and the red and blue segments represent the valid legs sampled in warm clouds and ice clouds, respectively.

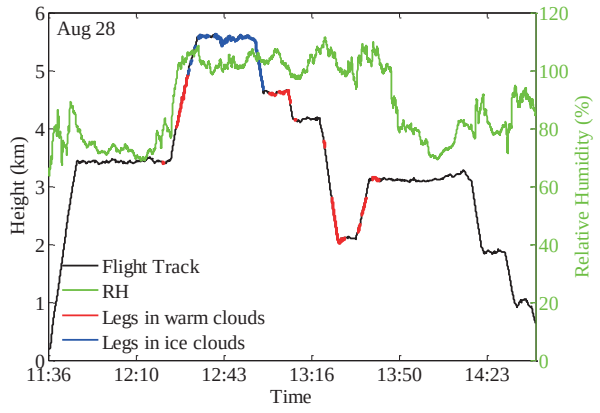

Fig. 2. Flight pattern for the 28 August case. The black line represents the track of the plane; the green line represents RH measured by CIP; and the red and blue segments represent the valid legs sampled in warm clouds and ice clouds, respectively.

According to the RH measured by CIP (the green line in Fig. 2), a portion of cloud in the flight was accurately selected.

4. Comparison of reflectivity obtained from aircraft and radar

4.1 *Reflectivity calculated from in situ measurements*

Two scatter modes, Rayleigh and Mie scattering, are applied to the backscattering of the millimeter-wave radiation caused by hydrometeors. Lhermitte (1990) pointed out that at 35 GHz, for particle diameters below 2.7 mm, the Rayleigh backscatter is within 3 dB of the Mie backscatter. In other words, the Rayleigh assumption is roughly valid for particles with a diameter smaller than 1 mm at Ka- band (Ellis and Vivekanandan, 2011). As a result, Rayleigh theory has been employed in many studies to calculate the reflectivity factor Z (mm^6 m^{-3}) from cloud and drizzle droplets at 35GHz. However, to gain more accuracy, Z was computed based on the Mie function in our study:

$$Z = \frac{10^6\lambda^4}{4\pi^5|K|^2}\int_0^{D_{\max}} N(D)\sigma_{\rm b}(D)dD\,, \qquad (1)$$

where $\sigma_{\rm b}$ (cm^2) is the Mie backscatter cross section, $|K|^2$ is the dielectric factor (with a value of 0.8797 for water and 0.176 for solid ice when calculating at 35 GHz), and $N(D)dD$ (m^{-3}) is the number concentration of particles with diameter between D and $D+dD$. Z is then denoted by $10\lg Z$ in a unit of dBZ. The reflectivity factor is generally referred as reflectivity in this study.

4.2 *Radar–aircraft comparisons*

Since the MMRC did not work properly on 29 August 2010, the simultaneous MMCR and aircraft observation data were taken from two flights, from 1240:46 to 1247:22 LST 28 August 2010 and from 1302:00 to 1342:25 LST 17 September 2010. The stratiform clouds were detected on both of these two days. The match in time was done simply by using the same times for data gathered by both sensors, and the flight patterns during the co-observation period are shown in Fig. 3. From this figure, it is clear that the cloud parcels sampled on the two days were moving towards the MMCR, as indicated by the wind direction. An assumption was adopted that the cloud properties did not change between the time when sampled by the aircraft and by the radar, typically a few minutes (Hogan et al., 2006). Thus, it is reasonable to evaluate the accuracy of the *in situ* measurements by comparing with the radar measurements.

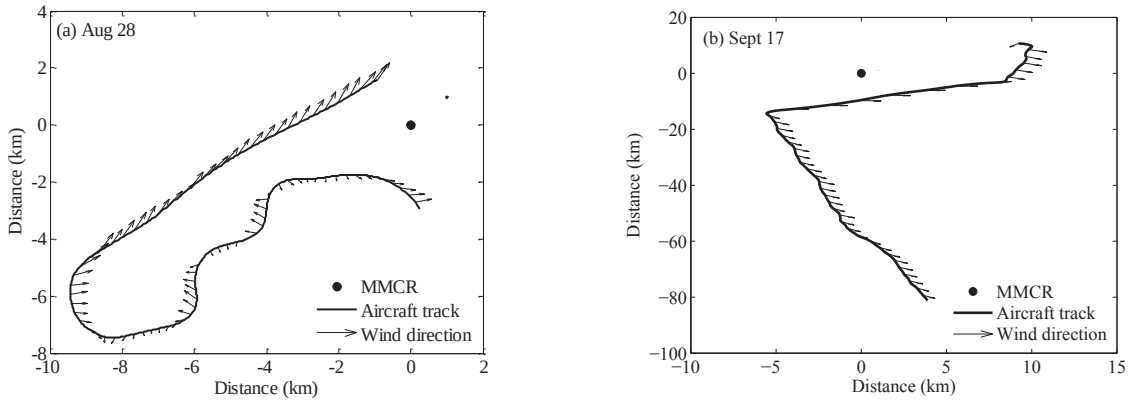

Fig. 3. (a) Flight pattern for the 28 August case during the co-observation period. The black dot shows the position of ground-based MMCR and the arrows represent the wind direction. (b) The same as (a), but for the 17 Sep case.

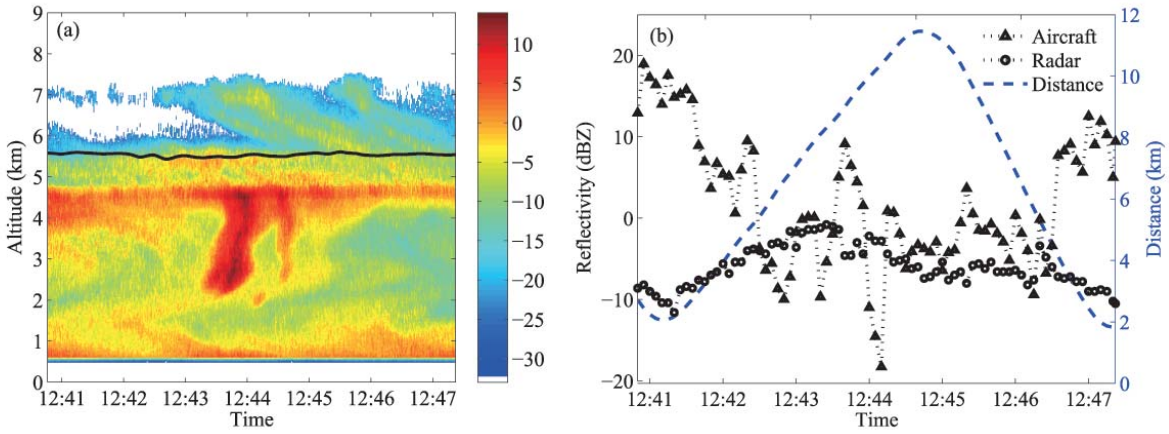

Fig. 4. (a) Radar reflectivity with the flight path superimposed for 28 August 2010. The black line indicates the track of the aircraft. (b) Reflectivity comparison between *in situ* measurements and MMCR, where the *in situ* data are represented by triangles and the MMCR data by circles. Both are averaged over a 5-s period. The blue dashed line represents the horizontal distance between the aircraft and MMCR.

In the 28 August case, the aircraft flew at an altitude of 5.5 km, spanning temperatures from −3°C to −2°C. The enhanced reflectivity field (bright band) below 5 km (in Fig. 4a) indicated melting and the existence of ice particles above. Also, the linear depolarization ratio (LDR) data from MMCR (not shown here) confirmed the presence of ice. Therefore, *in situ* reflectivity was calculated by employing the backscattering coefficient of ice particles, and to reduce the variance in number concentration, a five-second-averaged distribution spectrum was used instead of the DSD gathered in real time.

Figure 4a presents the reflectivity detected by MMCR, and the black line represents the track of the flight at the same time when MMCR collected the information. The radar reflectivities in the bins on the flight path were compared with the simultaneous *in situ* measurements, as shown in Fig. 4b. The blue dashed line indicates the horizontal distance between the two sensors. It can be seen from Fig. 4b that the agreement in this case was poor at the beginning and end of the co-observation period, when the two sensors coordinated well in terms of distance. The discrepancies in reflectivity became smaller in the middle period though the distance between the two sensors being greater. By a careful inspection of Fig. 4a, it is clear that the variation of deviation has a relationship with the portion of cloud in which the plane flew. The two sets of reflectivity results differed from each other to a large degree when data were collected at the cloud top. In contrast, the agreement between the two was relatively good when sampled inside the cloud.

Several factors were responsible for the deviation. The most significant one was the difficulty of exactly matching up the aircraft and radar samples due to imprecise collocation between the two sensors and their distinct sample volumes. The CAS and CIP probes had sample volumes of 25 cm^3 s^{-1} and 16 L s^{-1}, respectively, assuming an aircraft speed of 100 m s^{-1}. At an altitude of 5.5 km, the sample volume of MMCR was nine orders of magnitude greater than the CAS probe volume, and six orders of magnitude greater than the CIP volume. The large sample volume of MMCR would have led to a problem of an unfilled radar beam at the edge of the cloud (Brown and Illingworth, 1995). Nevertheless, the impact would have been minor due to the small gate space of MMCR (only 30 m). Besides, the cloud was spatially inhomogeneous, a feature that is known to be more intense at the cloud top than in the cloud, leading to the large deviation between the measured and *in situ* reflectivity when the data were collected at the top of the clouds. Other possible causes were the reduced precision of radar measurements at low signal-to-noise ratios, large uncertainties in both measurement platforms, and the attenuation caused by water droplets.

In the 17 September case, the aircraft flew at an altitude of 3.0 km, and temperatures detected at this height were all above 0°C. Therefore, this case comprised an all-water cloud and we calculated reflectivity assuming Mie scattering from water droplets. The collected spectra in this case were averaged over a 10-s time period. The reflectivities derived from both radar and calculations are shown in Fig. 5. Similar to the case of 28 August, over the initial period from 1302 to 1317 LST 17 September 2010, when sampling at the top of cloud, the *in situ* results were much higher and more fluctuated than the radar data. It is possible that the volume of the radar may have been averaging in clear air, thus revealing a lower reflectivity. After 1317 LST 17 September 2010, the plane was completely inside the cloud and the level of discrepancy became frequently smaller. From 1317 to 1323 LST 17 September 2010 in particular, the reflectivity measured by radar was quite comparable to that derived from aircraft measurements, and the two sets of reflectivity results generally followed a similar tendency. Then, along with the increase in distance, the differences between the two grew large again.

The RMSE for the reflectivity measured by MMCR and derived from DSD was calculated for the two cases with data gathered inside the cloud. Taking into account that a greater horizontal distance will result in less correlation between the two sets of reflectivity results, the data that were sampled over the period when the aircraft flew beyond 60 km of the MMCR on 17 September were eliminated. The resulting RMSE value was 6.1 dBZ for the 28 August case, and 5.5 dBZ for the 17 September case, indicating that the discrepancy in reflectivity was a little larger for the former. This larger bias could be ascribed to the algorithm that was used to calculate the reflectivity from the DSDs. The ice particles were simply assumed to be solid spherical particles, regardless of their densities and habits. Moreover, the cloud was actually mixphased, rather than an all-ice cloud. The average number concentration of cloud droplets was 163 cm^{-3}, with a maximum value of 587.4 cm^{-3}, and the liquid water content was up to 0.25 g m^{-3} in the co-observation period. According to Hobbs et al. (1980) a high density of particles occurs only when supercooled water is present. The liquid water will induce rimming, which

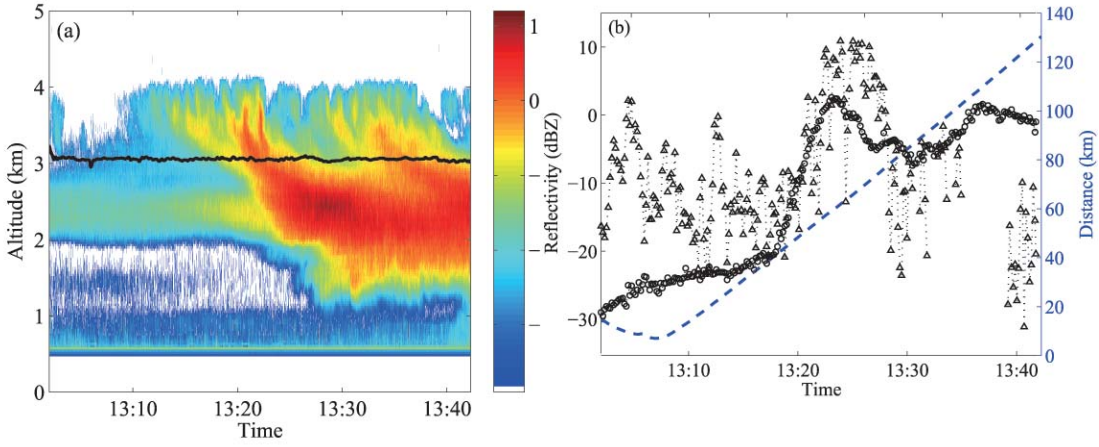

Fig. 5. The same as Fig. 4, but for the case on 17 September 2010. The two kinds of reflectivity are averaged over a 10-s period.

not only promotes the growth of ice but also increases particle density. This may explain why the calculated reflectivity was lower than the value measured by radar in some time intervals (see Fig. 4b). On the whole, the reflectivities obtained from MMCR and measured DSD were comparable when both instruments were close in time and space, which validates the accuracy of aircraft-derived radar reflectivity values and, further, substantiates the feasibility of a radar-based description of microphysical characteristics.

5. Data application

5.1 *Threshold reflectivity for drizzle*

5.1.1 *Definition of drizzle*

Generally, two size ranges are adopted to define drizzle in most studies. One common criterion uses a diameter of 50 μm to discriminate cloud droplets and drizzle (e.g. Frisch et al., 1995; French et al., 2000). The classification depends on different droplet growth mechanisms. Droplets smaller than 40 μm in diameter grow mainly through condensation, while growth of larger droplets is dominated by coalescence (Cober et al., 1996). Another definition restricts drizzle size to a range of 200–500 μm in diameter (Sauvageot and Omar, 1987), a definition that is based on the relationship between size and terminal velocity. The terminal velocity of droplets with a diameter smaller than 200 μm is negligible, and droplets larger than 500 μm in diameter are quite likely to reach the ground, thus being referred to as raindrops. The latter definition of drizzle was employed in this study because droplets with a diameter larger than 200 μm were very common in our observations.

The combined DSDs altogether had 76 bins. Droplets detected in the first 22 bins were considered to be cloud particles, whereas those from the 23rd to 76th bins were used to determine drizzle presence. If there were no droplets measured in the last 54 bins in one sampling period, this cloud sample was classified as a drizzle-free case; otherwise, a drizzle case.

5.1.2 *Statistical method*

In order to find out the threshold reflectivity to diagnose drizzle and cloud particles for MMCR, the probability distribution functions (PDFs) of reflectivity due to drizzle and drizzle-free data were calculated individually from combined observed DSDs by utilizing Mie Theory, as mentioned in section 4. Because the cloud droplet size distribution spectra and related microphysical properties are determined by different mechanisms in horizontal and vertical directions (Liu et al., 2008), only horizontal flight legs were investigated in this part of the study. Legs that contained scarce drizzle records were rejected to ensure sufficient statistics. Besides, records sampled at temperatures below 0°C were also excluded in case of ice particles.

Two statistical methods proposed by Wang and Geerts (2003) were adopted to find out the threshold and are briefly described here. For reflectivities of drizzle and cloud droplets, there is an overlapped part in most cases (see Fig. 6), meaning the reflectivity corresponding to the cross point of the two PDFs can be chosen as the threshold. It should be noted that this method is sensitive to the sample number and the bin width, with more samples and a broader bin width leading to smoother PDFs. Therefore, sometimes the PDFs may fluctuate intensively and there is more than one cross point in the PDFs (Fig. 6b). In such a situation, this method tends to fail.

The second method is to calculate a coefficient called the "hit rate" to determine the drizzle reflectivity threshold, defined as:

$$H = (n_{00} + n_{11})/n \, . \tag{2}$$

In this method, a value of reflectivity is selected to be a threshold in advance. If a sample contains no drizzle and the reflectivity pertaining to this sample is below the assumed threshold, then this sample is included into n_{00}. Equally, n_{11} consists of samples which are with drizzle and have a reflectivity exceeding the assumed threshold. The value of n is the total number of samples in one case. After utilizing this method on a series of assumed threshold reflectivities between -20 and -5 dBZ, the one corresponding to the maximum hit rate was considered to be the optimal threshold.

5.1.3 *Results*

Some of the PDFs of reflectivity are displayed in Fig. 6. It is clear that the two kinds of PDFs separated well from each other, merging together only within a small part. The upper limits of Z for drizzle-free cloud varied between -10 and -5 dBZ, while the lower limits of Z for drizzle were above -20 dBZ, or even -10 dBZ. Therefore, it was reasonable for us to expect a threshold of reflectivity that can discriminate with-drizzle cloud from drizzle-free cloud.

The two types of threshold are indicated by vertical lines in Fig. 6. The dashed and solid lines demonstrate the value determined by the cross point and hit rate methods, respectively. The differences between the two kinds of thresholds were quite acceptable, the maximum occured in a case of a leg on 17 September (see Fig. 6c) and was within 2.5 dBZ, thus verifying the reliability of defining a reflectivity threshold for drizzle. We then defined the mean value of the two thresholds to be the ultimate threshold. It can be seen that, despite the two flights having undergone different syn-

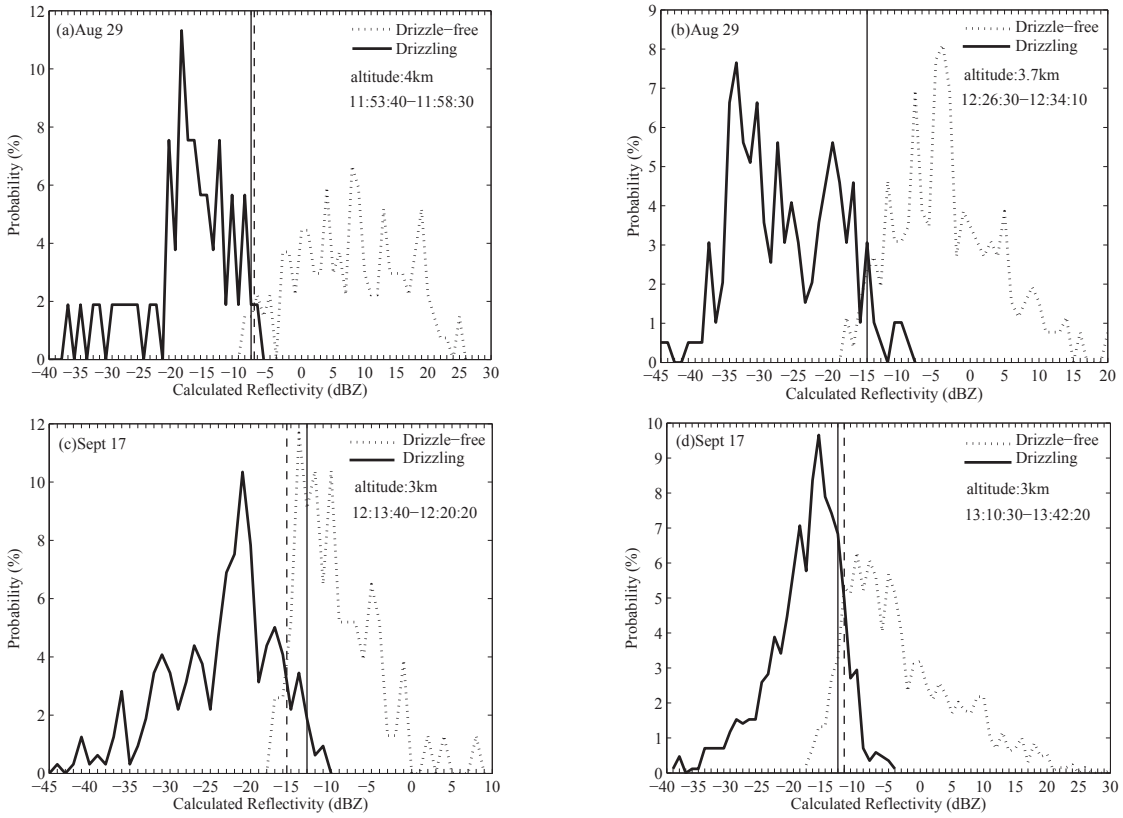

Fig. 6. Probability of *in situ* calculated reflectivity for drizzle and drizzle-free cases. The solid and dashed curve lines represent drizzle-free and drizzle cases, respectively. The dashed straight lines show the cross value of the two probability curves. The solid vertical line is the threshold reflectivity determined by the hit rate method.

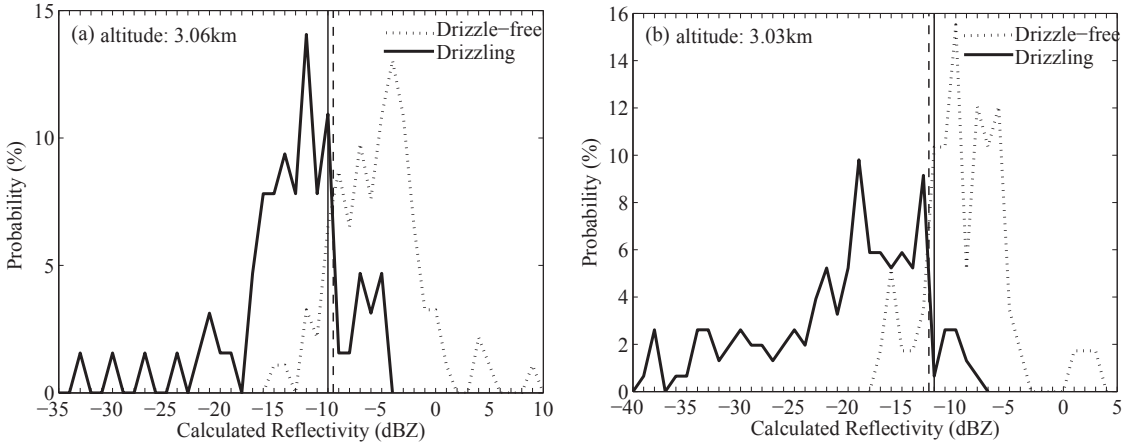

Fig. 7. The same as Fig. 6, but for a section of the flight containing three horizontal legs at different heights on 17 September 2010.

optic conditions, and data having been collected in different parts of the cloud, thresholds derived from these flight legs showed good agreement, almost spanning from −15 to −12dBZ, except a leg on 29 August shown in Fig. 6a. Wang and Geerts (2003) studied reflectivity of drizzle-containing and drizzle-free clouds at different cloud altitudes and concluded that the threshold and the merging of reflectivity PDFs are both height-dependent, increasing monotonically from cloud base to cloud top. A section of the flight on 17 September, which contained two horizontal legs at different heights, was selected and the PDFs of reflectivity plotted, as shown in Fig. 7. It can be seen that there was indeed a correlation between height and threshold. As the aircraft crossed the cloud at altitudes of 3.06 and 3.03 km, the corresponding threshold was about −10 and −12 dBZ, respectively. This may be one explanation for the disparities of thresholds. However, owing to the lack of complete macrostructural information of the cloud, we unfortunately cannot further prove the relationship between threshold and altitude here.

5.2 *Relationship between Z and LWC*

Deriving the liquid water content of water clouds from cloud radar reflectivity can be achieved simply by applying a relationship between reflectivity and LWC. Both reflectivity and LWC are calculated from airborne DSD measurements, and then linked together by fitting the scattering data. A form of power law is commonly deployed to express the Z–LWC relationship:

$$Z = aM^b \,, \tag{3}$$

where M stands for LWC, a and b are regression parameters. Some published Z–LWC relationships are listed in Table 1. The first three relationships between LWC and radar reflectivity are only valid for clouds without drizzle-sized drops and the last two are for clouds containing drizzle. Whether drizzle-free or with-drizzle cloud, there are no consistent correlations between LWC and reflectivity because of the different size distributions and physical mechanisms (Khain et al., 2008).

This section is concerned with Z–LWC relation calculated from samples taken from horizontal legs in order to avoid the impact of different mechanisms in horizontal and vertical directions. The relationship of Z and LWC is shown as a scattergram in Fig. 8. Both the drizzle-free and drizzle-containing partitions were taken into account, represented by the red and blue points, respectively. A clear relation exists between Z and LWC when there were no drizzle droplets.. However, points calculated from the drizzle partition are dispersed widely and thus a correlation between Z and LWC was not evident. The scatter brought about by drizzle was excluded according to two criteria. One was based on Gerber's (1996) investigation on microphysical properties of drizzling clouds, who concluded that a threshold of r_e of 16 μm can be used to identify heavy drizzles. The other was a ratio between radar reflectivity and the extinction coefficient Z/α, for which a logarithmic value of 1.8 indicates the existence of heavy drizzle (Krasnov and Russchenberg, 2005). The extinction coefficient α is defined as:

$$\alpha = 2\pi \sum N_i r_i^2 \times 10^{-6} \,, \tag{4}$$

where N_i is the number of particles measured in the ith bin, and r_i is the mid-radius of the ith bin and in a unit of mm.

The diamonds in Fig. 8 show the DSDs with r_e<16 μm but lg(Z/α)⩾1.8, which are filtered out. Consequently, deviating points were considerably reduced.

The classical form of power law was adopted to express the Z–LWC relationship. By regressing with the least-squares method, relations were derived as follows: $Z = 3.77\times \mathrm{M}^{1.22}$, for cloud without drizzle; and $Z = 46.08\times \mathrm{M}^{1.6}$, for cloud containing drizzle.

Although the values of b in the two relationships were similar to previous studies, the values of a deviated a lot from published values. One possible explanation for this is related to the definition of drizzle we adopted in our study. We categorized droplets into cloud particles with a diameter below 200 μm, rather than 50 μm. Another likely explanation is the high degree of spatial variability of DSD in different regions and different types of clouds (Deng et al., 2009), hence inducing different microphysical properties.

Table 1. Regression parameters of the Z–LWC relationship using *in situ* measurements.

	a	b	Cloud type
Sauvageot and Omar (1987)	0.030	1.31	non or very weakly precipitating stratocumulus and cumulus
Fox and Illingworth (1997)	0.012	1.16	non precipitating marine stratocumulus
Wang and Geerts (2003)	0.044	1.34	non precipitating marine stratus
Baedi et al. (2000)	57.544	5.17	stratocumulus with light drizzle
Krasnov and Russchenberg (2005)	323.59	1.58	stratiform clouds with heavy drizzle

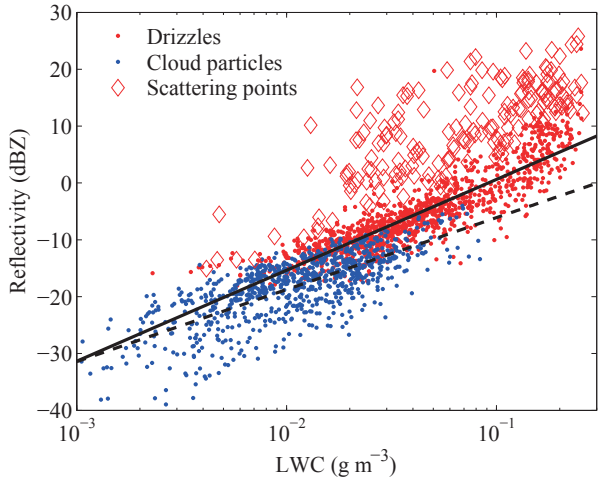

Fig. 8. Scattergram of reflectivity versus LWC, computed from the combined DSDs on horizontal flight legs. The blue and red dots are for drizzle-free and drizzle cases, respectively. The diamonds are the scatter points as a result of drizzle drops and were filtered out. The fitted Z–LWC relationships are represented by the dashed line for cloud particles and the solid line for drizzle drops.

6. Summary

Along with the development of millimeter-wavelength radar, it is valuable to study microphysical characteristics of clouds by remote sensing methods, which can give wide coverage in both time and space with low cost. Observations of clouds through a combination of aircraft measurements and a 35-GHz cloud radar took place over Yitong, Jilin Province, China, in 2010, the results of which provided a good opportunity to retrieve radar-based cloud microphysics.

The airborne measurements were used to calculate reflectivity according to Mie theory. The comparison between the calculated reflectivity and the value measured directly by MMCR showed that: (1) in both water and ice cloud the results were in good agreement when the aircraft collected data inside the cloud and had a good spatial collocation with the ground-based MMCR; and (2) in ice cloud they showed a relatively large deviation thought to result from the occurrence of liquid water in the cloud. The RMSE values for the two reflectivities were 5.5 dBZ for the water cloud case and 6.1 dBZ for the ice cloud case. The discrepancy may have been due to several factors, including the inconsistent sample volumes of airborne probes and radar, different regions detected by the two sensors, incomplete filling of range gates of MMCR, and uncertainties in *in situ* measurements and reflectivity retrievals. Nevertheless, the level of agreement in warm cloud confirmed the accuracy of both *in situ* and radar measurements and made it possible to derive relations between reflectivity and cloud microphysical properties based on the aircraft data collected during this flight.

One relation of interest in this paper was the threshold reflectivity above which drizzle drops are prone to be present. Drizzle drops were identified by the CPI probe, and the calculated reflectivity showed drizzle was unlikely to present below −20 dBZ. There was just a small overlap between the two PDFs of reflectivity due to cloud particles and drizzle drops, indicating the existence of the threshold. Two different statistical methods were deployed to obtain this threshold, and it was found that both of them achieved similar values, within a difference of 2.5 dBZ. Their average was used as the ultimate threshold. For most cases, these thresholds varied in a range of −15 to −12 dBZ, regardless of the synoptic conditions, and were close to those reported in previous studies.

The relationship between reflectivity and LWC was also provided. Unlike traditional studies on this subject, the entire DSD spectra were investigated, involving cloud partitions containing drizzle droplets. In comparison to cloud particles, drizzle drops brought about many scatter points to the Z–LWC diagram and, as a result, the derivation of a Z–LWC relation for drizzling cases was not as straightforward as drizzle-free cases. It appears that most of these scatter points were related to particles with large Z/α ratios (logarithm value $\geqslant$1.8) but small r_e (<16 μm). After removing these scatters, the correlation of Z–LWC for drizzle cases became much more evident and empirical Z–LWC relations for both types of case were regressed with the least-squares method.

Owing to the large variance in DSDs, there is no universal relationship that can capture the microphysical properties of cloud in different regions. With respect to cloud in a certain region, a more accurate empirical correlation should be derived from *in situ* data. Our work studied the threshold of precipitation and the Z–LWC relationship from two flights over Northeast China. There were deviations between our retrievals and previously published results, which were concerned with stratus and stratocumulus clouds in European and North American areas. So far, this work can largely be considered as exploratory, mainly because of the small number of sampling data and lack of information about cloud macroscopic properties. More data are needed to evaluate and correct the relations between reflectivity and cloud parameters derived in this paper. Additionally, there is a need for future work aimed at understanding the effects of the physical mechanisms that lead to the differences in the relationships.

Acknowledgements. The authors are grateful to the Weather Modification Office of Jilin Meteorological Bureau for providing the aircraft data. We also thank the Laboratory of Cloud-Precipitation Physics and Severe Storms, Institute of Atmospheric Physics, for helpful information on instrumentation. This work was supported by the National Key Program for Developing Basic Sciences under Grant 2012CB417202 and the National Natural Science Foundation of China under Grant Nos. 40975014, 41030962 and 41175038. This work was also sponsored by the Program for Postgraduates Research Innovation of Jiangsu Higher Education Institutions (Grant No. CXZZ11-0615).

REFERENCES

Baedi, R., J. J. M. de Wit, H. W. J. Russchenberg, J. S. Erkelens, and J. P. V. Poiares Baptista, 2000: Estimating effective radius and liquid water content from radar and lidar based on the CLARE98 dataset. *Phys. Chem. Earth* (B), **25**(10–12), 1057–1062.

Baumgardner, D., H. Jonsson, W. Dawson, D. O'Connor and R. Newton, 2001: The cloud, aerosol and precipitation spectrometer: A new instrument for cloud investigations. *Atmospheric Research*, **59–60**, 251–264.

Brown, P. R. A., and A. J. Illingworth, 1995: The role of spacebome millimeter-wave radar in the global monitoring of ice cloud. *J. Appl. Meteor.*, **34**, 2346–2366.

Chin, H. N. S., D. J. Rodriguez, R. T. Cederval, C. C. Chuang, A. S. Grossman, and J. J. Yio, 2000: A microphysical retrieval scheme for continental low-level stratiform clouds: Impacts of subadiabatic character on microphysical properties and radiation budgets. *Mon. Wea. Rev.*, **128**, 2511–2527.

Cober, S. G., J. W. Strapp, and G. A. Isaac, 1996: An example of supercooled drizzle drops formed through a collision-coalescence process. *J. Appl. Meteor.*, **35**, 2250–2260.

Comstock, K. K., C. S. Bretherton, and S. E. Yuter, 2005: Mesoscale variability and drizzle in Southeast Pacific stratocumulus. *J. Atmos. Sci.*, **62**, 3792–3807.

Deng, Z. Z., C. S. Zhao, Q. Zhang, M. Y. Huang, and X. C. Ma, 2009: Statistical analysis of microphysical properties and the parameterization of effective radius of warm clouds in Beijing area. *Atmospheric Research*, **93**, 888–896.

Ellis, S. M., and J. Vivekanandan, 2011: Liquid water content estimates using simultaneous S and Ka band radar measurements. *Radio Sci.*, **46**, RS2021, doi: 10.1029/2010RS004361.

Fox, N. I., and A. J. Illingworth, 1997: The retrieval of stratocumulus cloud properties by ground-based cloud radar. *J. Appl. Meteor.*, **36**, 485–492.

French, J. R., G. Vali, and R. D. Kelly, 2000: Observations of microphysics pertaining to the development of drizzle in warm, shallow cumulus clouds. *Quart. J. Roy. Meteor. Soc.*, **126**, 415–443.

Frisch, A. S., C. W. Fairall, and J. B. Snider, 1995: Measurement of stratus clouds and drizzle parameters in ASTEX with a Ka-band Doppler radar and a microwave radiometer. *J. Atmos. Sci.*, **52**, 2788–2799.

Gerber, H. 1996: Microphysics of marine stratocumulus clouds with two drizzle modes. *J. Atmos. Sci.*, **53**(12), 1649–1662.

Hobbs, P. V., T. J. Matejka, P. H. Herzegh, J. D. Locatelli and R. A. Houze, 1980: The mesoscale and microscale structure and organization of clouds and precipitation in midlatitude cyclones. I: A case study of a cold front. *J. Atmos. Sci.*, **37**, 568–596.

Hogan, R. J., M. P. Mittermaier, and A. J. Illingworth, 2006: The retrieval of ice water content from radar reflectivity factor and temperature and its use in evaluating a mesoscale model. *J. Appl. Meteor. Climatol.*, **45**, 301–317.

Khain, A., M. Pinsky, L. Magaritz, O. Krasnov, and H. W. J. Russchenberg, 2008: Combined observational and model investigations of the Z–LWC relationship in stratocumulus clouds. *J. Appl. Meteor. Climatol.*, **47**, 591–606, doi: 10.1175/2007JAMC1701.1.

Kogan, Z. N., D. B. Mechem, and Y. L. Kogan, 2005: Assessment of variability in continental low stratiform clouds based on observations of radar reflectivity. *J. Geophys. Res.*, **110**, D18205, doi: 10.1029/2005JD006158.

Kollias, P., B. A. Albrecht, and F. Marks Jr, 2002: Why Mie? Accurate observations of vertical air velocities and raindrops using a cloud radar. *Bull. Amer. Meteor. Soc.*, **83**(10), 1471–1483.

Kollias, P., E. E. Clothiaux, M. A. Miller, B. A. Albrecht, G. L. Stephens, and T. P. Ackerman, 2007: Millimeter-wavelength radar: New frontier in atmospheric cloud and precipitation research. *Bull. Amer. Meteor. Soc.*, **80**(10), 1608–1624, doi: 10.1175/BAMS-88-10-1608.

Krasnov, O. A., and H. W. J. Russchenberg, 2005: A synergetic radar-lidar technique for the LWC retrieval in water clouds: Description and application to the Cloudnet data. 32*nd Conf. on Radar Meteorology*, Albuquerque, NM, AMS R. **11**.

Kropfli, R. A., and R. D. Kelly, 1996: Meteorological research applications of MM-wave radar *Meteor. Atmos. Phys.*, **59**, 105–121.

Lawson, R. P., and P. Zuidema, 2009: Aircraft microphysical and surface-based radar observations of summertime arctic clouds. *J. Atmos. Sci.*, **66**, 3505–3529.

Lhermitte, R., 1990: Attenuation and scattering of millimeter wavelength radiation by clouds and precipitation. *J. Atmos. Oceanic Technol.*, **7**, 464–479.

Liu, Y., P. H. Daum, S. S. Yum, and J. Wang, 2008: Use of microphysical relationship to discern growth/decay mechanisms of cloud droplets with focus on Z–LWC relationships. 15*th International Conference on Clouds and Precipitation*, Cancun, Mexico.

Morales, J., J. Trabal, S. L. Cruz-Pol, and S. M. Sekelsky, 2004: Cirrus clouds Millimeter-wave reflectivity comparison with *in situ* ice crystal airborne data.

Fourth International Asia-Pacific Environmental Remote Sensing Symposium 2004: Remote Sensing of the Atmosphere, Ocean, Environment, and Space. International Society for Optics and Photonics, 75–83.

Paluch, I. R., C. A. Knight, and L. J. Miller, 1996: Cloud liquid water and radar reflectivity of nonprecipitating cumulus clouds. *J. Atmos. Sci.*, **53**, 1587–1603.

Sassen, K., G. G. Mace, Z. Wang, M. R. Poellot, S . M. Selensky, and R. E. McIntosh, 1999: Continental stratus clouds: A case study using coordinated remote sensing and aircraft measurements. *J. Atmos. Sci.*, **56**, 2345–2358.

Sauvageot, H., and J. Omar, 1987: Radar reflectivity of cumulus clouds. *J. Atmos. Oceanic. Technol.*, **4**, 264–272.

Slingo, A., 1990: Sensitivity of the earth's radiation budget to changes in low clouds. *Nature*, **343**, 49–51.

Wang, J., and B. Geerts, 2003: Identifying drizzle within marine stratus with W-band radar reflectivity. *Atmospheric Research*, **69**, 1–27.

Zhong, L. Z, L. P. Liu, S. Feng, R. S. Ge, and Z. Zhang, 2011: A 35-GHz polarimetric Doppler radar and its application for observing clouds associated with Typhoon Nuri. *Adv. Atmos. Sci.*, **28**(4), 945–956, doi: 10.1007/s00376-010-0073-5.